Yuzuncu Yil University
Journal of the Institute of Natural & Applied Sciences
https://dergipark.org.tr/en/pub/yyufbed

Research Article

Biogenic Synthesis, Characterization and Degradation of Methylene Blue Dye of Zinc Oxide Nanoparticles from Different Zinc Salts Using *Cinnamomum verum* Extract

Burcu AYDOĞDU*[1], İlkay ÜNAL[2]

[1]Munzur University, Faculty of Engineering, Department of Mechanical Engineering, 62000, Tunceli, Türkiye
[2]Munzur University, Faculty of Fine Arts, Design and Architecture Education, Department of Gastronomy and Culinary Arts, 62000, Tunceli, Türkiye
Burcu AYDOĞDU, ORCID No: 0000-0002-3309-1995, İlkay ÜNAL, ORCID No: 0000-0002-1587-4187
*Corresponding author e-mail: burcuaydogdu@munzur.edu.tr

Article Info

Received: 20.07.2024
Accepted: 11.11.2024
Online December 2024

DOI:10.53433/yyufbed.1518986

Keywords
Biogenic,
DPPH,
Methylene blue dye,
Total phenolic content,
Zinc oxide nanoparticle

Abstract: In this study, zinc oxide nanoparticles (ZnONPs) were synthesized using Cinnamomum verum extract from different zinc salts such as zinc acetate, zinc nitrate, zinc sulfate, and zinc chloride. The synthesized ZnONPs were characterized using X-ray diffraction (XRD), dynamic light scattering (DLS), Fourier transform infrared spectroscopy (FT-IR), and transmission electron microscopy (TEM). Additionally, The photocatalytic activities of ZnO nanoparticles were tested in the presence and absence of sunlight. Cinnamomum verum extract was analyzed for DPPH radical scavenging activity and total phenolic content (TPC). The study results showed that the type of zinc salt used significantly affects the morphology, size, and crystal structure of the ZnO nanoparticles. ZnONPs synthesized from zinc acetate (ZnONPsA) showed superior photocatalytic activity in the presence and absence of sunlight.

Cinnamomum verum Ekstraktı Kullanılarak Farklı Çinko Tuzlarından Elde Edilen Çinko Oksit Nanopartiküllerinin Biyojenik Sentezi, Karakterizasyonu ve Metilen Mavisinin Bozunması

Makale Bilgileri

Geliş: 20.07.2024
Kabul: 11.11.2024
Online December 2024

DOI:10.53433/yyufbed.1518986

Anahtar Kelimeler
Biyojenik,
Çinko oksit nanopartikül,
DPPH,
Metilen mavisi boyası,
Toplam fenolik içerik

Öz: Bu çalışmada çinko asetat, çinko nitrat, çinko sülfat ve çinko klorür gibi farklı çinko tuzlarından Cinnamomum verum ekstraktı kullanılarak çinko oksit nanopartikülleri (ZnONP'ler) sentezlendi. Sentezlenen ZnONP'ler, X-ışını kırınımı (XRD), dinamik ışık saçılımı (DLS), Fourier dönüşümü kızılötesi spektroskopisi (FT-IR) ve transmisyon elektron mikroskobu (TEM) kullanılarak karakterize edildi. Ayrıca ZnO nanopartiküllerinin fotokatalitik aktiviteleri güneş ışığının varlığında ve yokluğunda test edildi. Tarçın ekstraktı DPPH radikal temizleme aktivitesi ve toplam fenolik içerik (TPC) açısından analiz edildi. Çalışma sonuçları, kullanılan çinko tuzunun türünün ZnO nanopartiküllerinin morfolojisini, boyutunu ve kristal yapısını önemli ölçüde etkilediğini gösterdi. Çinko asetattan (ZnONPsA) sentezlenen ZnONP'ler her iki durumda da üstün fotokatalitik aktivite gösterdi.

1.Introduction

Nanotechnology has wide applications in many fields, including medicine, electronics, environmental science, and materials engineering, as it involves the design, production, and application of materials, devices, and systems at the nanometer scale (Naiel et al., 2022). Nanoparticles exhibit several important properties that make them so interesting such as their high surface-to-volume ratio, chemical reactivity, optical properties. These feature make nanoparticles more reactive than bulk materials (Khan et al., 2019). Zinc oxide (ZnO) nanoparticles, one of the most important functional nanoparticles, are a semiconductor with a high exciton energy (60 meV) and a wide band gap (3.37 eV)

(Bhandari et al., 2023).Zinc oxide (ZnO) nanoparticles have attracted great attention due to their various uses in electronics, optoelectronics, catalysis and biomedical applications (Sajid & Płotka-Wasylka, 2020; Zhou et al., 2023). ZnO nanoparticles have outstanding properties such as high surface area, chemical stability, photocatalytic activity, and biocompatibility, making them ideal candidates for sunscreens, antimicrobial coatings, and wastewater treatment applications (Fahmy et al., 2016; Tănase et al., 2021). Methylene blue (MB) dye is used as an important model pollutant in water pollution and environmental cleanup. MB is a synthetic dye widely used in the textile industry and other industries and is soluble in water. Effective and sustainable methods are needed to reduce the environmental impacts of such organic pollutants (Venkatesan et al., 2022; Fito et al., 2023). In addition, ZnO nanoparticles exhibiting variable morphologies have a very strong antibacterial effect on gram-negative and gram-positive bacteri (Sirelkhatim et al., 2015). Nanoparticles can be synthesized using physical, chemical, and biological methods. Physical and chemical synthesis of nanoparticles involves methods like ball milling, laser ablation, and sol-gel processes; however, these methods come with disadvantages such as high costs, requiring special equipment and potential environmental and health risks from toxic chemicals (Iravani et al., 2014; Nyabadza et al., 2023). In recent years, green synthesis of nanoparticles has emerged as a sustainable alternative by using natural sources to reduce metal salts into nanoparticles. This method uses natural sources such as plant extracts, microorganisms, and even biowaste to reduce metal ions to their nanoparticle form (Kulkarni et al., 2023; Osman et al., 2024). Plant extracts are widely used for nanoparticle synthesis due to several advantages. This process is environmentally friendly as well as cost effective, using the rich phytochemical composition of plants as reducing, coating and stabilizing agents (Kazemi et al., 2023). Gold (Au), silver (Ag), platinum (Pt), palladium (Pd), zinc oxide (ZnO), titanium dioxide (TiO_2), copper oxide (CuO) and iron oxide (Fe_3O_4) are synthesized from biological resources like plant extracts, which act as reducing and stabilizing agents (Zuhrotun et al., 2023; Aigbe & Osibote, 2024; Prabu & Losetty, 2024; Saod et al., 2024). *Cinnamomum verum* is widely used in traditional medicine due to its medicinal properties. *Cinnamomum verum* plants are rich in bioactive compounds such as polyphenols, flavonoids, and terpenoids, which exhibit potent antioxidant and antimicrobial activities (Błaszczyk et al., 2021; Das et al., 2022). These phytochemicals are effective in the synthesis of zinc oxide nanoparticles (ZnONPs). Despite the extensive literature on the effect of synthesis parameters on ZnO formation, the role of synthesis parameters in the evolution of ZnO photocatalytic properties is still not fully understood. Catalysis is a photochemical oxidative process in which the semiconductor surface is activated by UV light and produces free radicals (Prasad et al., 2020). Factors such as the synthesis method, the presence of surface contaminants, and counterions from the precursors used in the synthesis affect the catalytic activity of the material. In addition, a relationship needs to be established between synthesis parameters, morphological properties, and photocatalytic activity of ZnO particles (Rezapour & Talebian, 2011).

This study investigated the synthesis of ZnONPs by biogenic synthesis method with different zinc salts and the synthesis parameters were correlated with the photocatalytic activity of the material using MB degradation as a probe reaction. The precipitation method and different precursor salts were investigated for the photoactivity of the products. *Cinnamomum verum* extract was also used as a substrate for biological synthesis. The aim of this study was to gain a better understanding of how the synthesis method affects the structural, morphological and photocatalytic activity of ZnO in determining their roles.

2. Materials and Methods

2.1. Materials

All chemicals used in the study were of analytical grade and did not undergo any further purification. Zinc acetate ($Zn(CH_3CO_2)_2{\cdot}2H_2O$, 98%), Zinc Nitrate ($Zn(NO_3)_2.6H_2O$, 98%), Zinc Sulfate ($ZnSO_4{\cdot}7H_2O$, 99%), Zinc Chloride ($ZnCl_2$, 85%), Potassium hydroxide (KOH, 85%) were obtained from Sigma-Aldrich. The Cinnamomum verum was purchased from the local market.

2.2. Preparation of plant extract

Cinnamomum verum purchased from the spice shop was washed thoroughly with distilled water to remove impurities. The extract concentration was prepared by dissolving 0.5 g of the plant material

in 50 mL of distilled water, and then incubated at 40°C for 24 hours. The extract was then filtered through white band filter paper and kept at 4°C (Aydoğdu et al., 2024).

2.3. Determination of antioxidant activity /capacity of Cinnamomum verum extract

2.3.1. DPPH (2,2-diphenyl-1-picrylhydrazyl) assay

DPPH assay is a widely used method to measure the antioxidant capacity. This method is based on the reduction of the free form of DPPH, which is a radical, in the presence of antioxidants (Kedare & Singh, 2011). DPPH assay was performed according to the Marin-Flores et al. (2021) method (Marin-Flores et al., 2021). Briefly, 2.9 mL of DPPH reagent (0.1 mM in ethanol) was added to 0.1 mL of *Cinnamomum verum* extract or standard and mixed vigorously. The reaction mixture was stored in the dark at room temperature for 30 min, and the color change of DPPH was measured against a blank at 518 nm using UV-Vis spectrophotometer. Calibration was performed with six Trolox standards in the range of 5-100 mg/L. Linear calibration curves were drawn with R^2=0.9982R^2 = 0.9982R^2=0.9982 (Figure 1), and the results were calculated as Trolox equivalents per gram of dry sample. The percentage of inhibition was calculated using the following formula:

$$\text{Inhibition } \% = \frac{A_{\text{(control)}} - A_{\text{(test sample)}}}{A_{\text{(control)}}} \times 100 \quad (1)$$

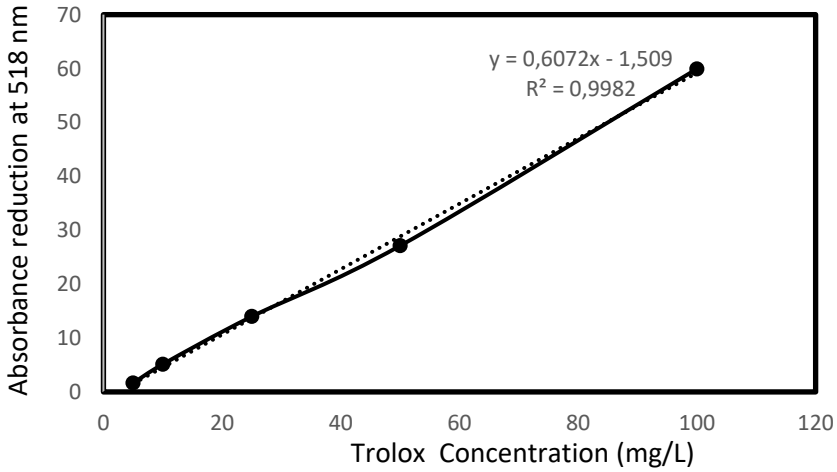

Figure 1. Trolox concentration vs absorbance of DPPH standard curve.

2.3.2. Determination of total phenolic contents

Total phenolic contents (TPC) were determined according to Folin-Ciocalteu's methods (Libbey & Walradt, 1968). Firstly, 0.5 mL of *Cinnamomum verum* extract, 1 mL of 1N Folin-Ciocalteu reagent and 1 mL of 20% Na_2CO_3 (w/v) were mixed. Then, the mixture was incubated at room temperature for 2 hours and measured with a UV-Vis spectrophotometer at 765 nm. A calibration curve was determined in the concentration range of 25-1000 mg/mL (y = 0.00008x- 0.0068; R^2 = 0.9981; y is absorbance, x is gallic acid concentration). The results were given as mg gallic acid equivalent (GAE)/1 mg *Cinnamomum verum* extract.

2.4. Green synthesis of ZnONPs using diffrent zinc salts

ZnONPs were synthesized from four different zinc salts using *Cinnamomum verum* extract. 25 mL of 0.1 M zinc salts solutions were prepared separately. 25 mL of 0.1 M zinc salt solutions were prepared separately and kept in a 60°C water bath for 1 hour. 25 mL of Cinnamomum verum extract was added to the zinc salt solutions and the pH was adjusted to 6 with 1 M KOH solution. The mixture was left in the shaking water bath at 60°C for another 2 hours. Then, the solution was centrifuged at 5000 rpm for 15 min, washed several times with distilled water, and dried in an oven at 40 °C for 24 h (Aydoğdu et al., 2024). Figure 2 shows the stages of ZnO nanoparticle synthesis synthesized from four different zinc salts using *Cinnamomum verum* extract and green synthesis mechanism for producing ZnO

nanoparticles. Biosynthesis nanoparticles were coded as ZnONPsC (chloride salt), ZnONPsA (acetate salt), ZnONPsS (sulphate salt), ZnONPsN (nitrate salt).

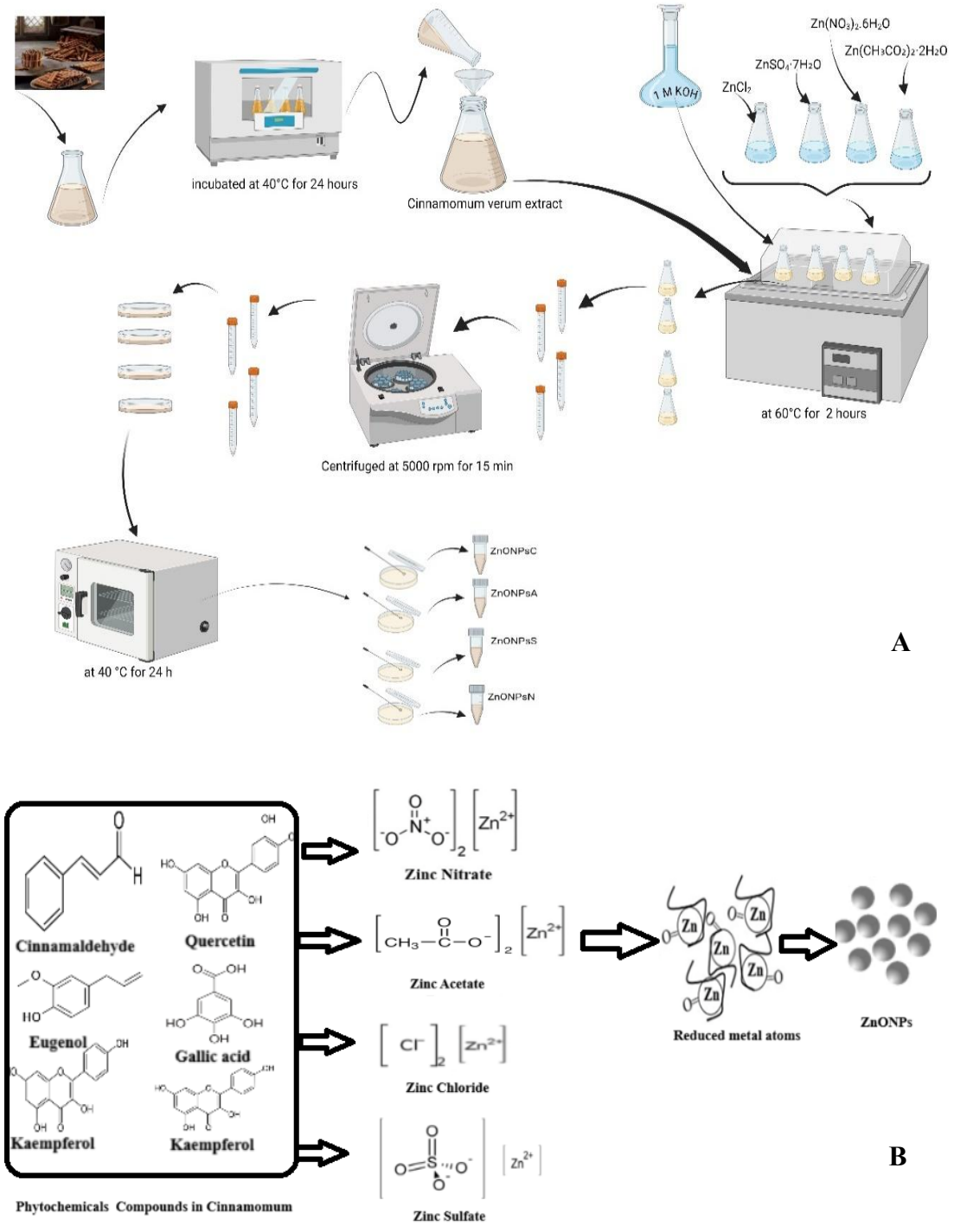

Figure 2. A) Schematic showing of ZnO NP synthesis from different zinc salts B) Green synthesis mechanism for producing ZnO nanoparticles.

2.5. Characterization of zinc oxide nanoparticles

X-ray diffractometer (XRD) was determined using Rigaku Miniflex (Japan) over the 2θ angle range from 20° to 80. Particle size and zeta potential value were determined using a Malvern Zetasizer

Nano ZSP. For Fourier transform infrared spectroscopy (FT-IR) analysis, ATR-FTIR 6700 Jasco (Japan) was used in the range of 4000–400 cm^{-1}. Structural feature of NPs was determined using transmission electron microscopy/TEM (JEOL Brand, JEM-1011). DPPH, TCP and methylene blue degradation measurements were determined by UV-Vis spectrophotometer (Shimadzu UV-1800).

2.5.1. Catalytic activity on degradation of methylene blue (MB) dye

The catalytic activity of the synthesized ZnO NPs was evaluated by MB degradation under direct sunlight and in the dark. 15 mL of MB (100 ppm, pH: 10) was placed in a beaker containing 15 mg ZnONPs. The mixture was stirred on a magnetic stirrer at 145 rpm for 90 minutes and then centrifuged at 5000 rpm for 5 minutes. The absorbance was measured with a UV-visible spectrometer at 664 nm and the photodegradation percentage of MB (photocatalytic efficiency of ZnO) in aqueous medium was calculated by the following equations:

$$\eta = \frac{(C_0 - C)}{C_0} \times 100 \quad (1)$$

where η is photodegradation percentage, C_0 is the initial dye concentration without catalyst and C is the final dye concentration with catalyst after 90 min (Saeed et al., 2015).

3. Results and Discussion

3.1. DPPH radical scavenging of *Cinnamomum verum* extract

The *Cinnamomum verum* extract with a concentration of 10 g/L that is DPPH free radical scavenging activity was found to be 128 mg/L, indicating its strong antioxidant properties. This high value suggests that Cinnamomum verum extract can effectively neutralize free radicals, making it a potent natural antioxidant source. Previous studies reported that *Ceylon Cinnamomum* showed 60.49 ± 0.48 to 107.69 ± 2.01 mg Trolox equivalent (Abeysekera et al., 2013). With a different approach, Sudan et al. performed DPPH radical scavenging assay of aqueous Cinnamon bark extracts and reported that they showed high radical scavenging activity with IC_{50} 122 mg/ml (Sudan et al., 2013).

3.2. Total Phenolic Contents of *Cinnamomum verum* extract

The total phenolic content of the *Cinnamomum verum* extract was found to be 290,62 mg Gallic Acid Equivalents per gram (mg GAE/g). This high phenolic content indicates that Cinnamomum verum extract is rich in phenolic compounds, which contribute significantly to its antioxidant properties. Song et al. (2010) measured the total phenolic content of 56 Chinese medicinal herbs by the Folin-Ciocalteu method. They determined that the plants had TPC values between 0.18 ± 0.01 and 59.43 ± 1.03 mgGAE/g (Song et al., 2010).

3.3. XRD results

The XRD results of ZnONPs synthesized with different salts are given in Figure 3. The XRD spectra of ZnONP samples showed an intense diffraction peak corresponding to (100), (002), (101), (102), (110), (103), (200), (112), (201), (004) and (202) planes (JCPDS 36-1451) (Talam et al., 2012) (Table 1). The average nanoparticle crystallite size was calculated from the XRD peak using the Debye-Scherrer equation. Crystallite size varied between samples. ZnONPsC had the smallest crystallite size (20.04 nm) and ZnONPsS was the largest (24.34 nm). The XRD data clearly shows that all four ZnO nanoparticle samples have similar crystallographic structures but differ in crystallite sizes. This variation could impact their physical and chemical properties (Abdullah et al., 2024).

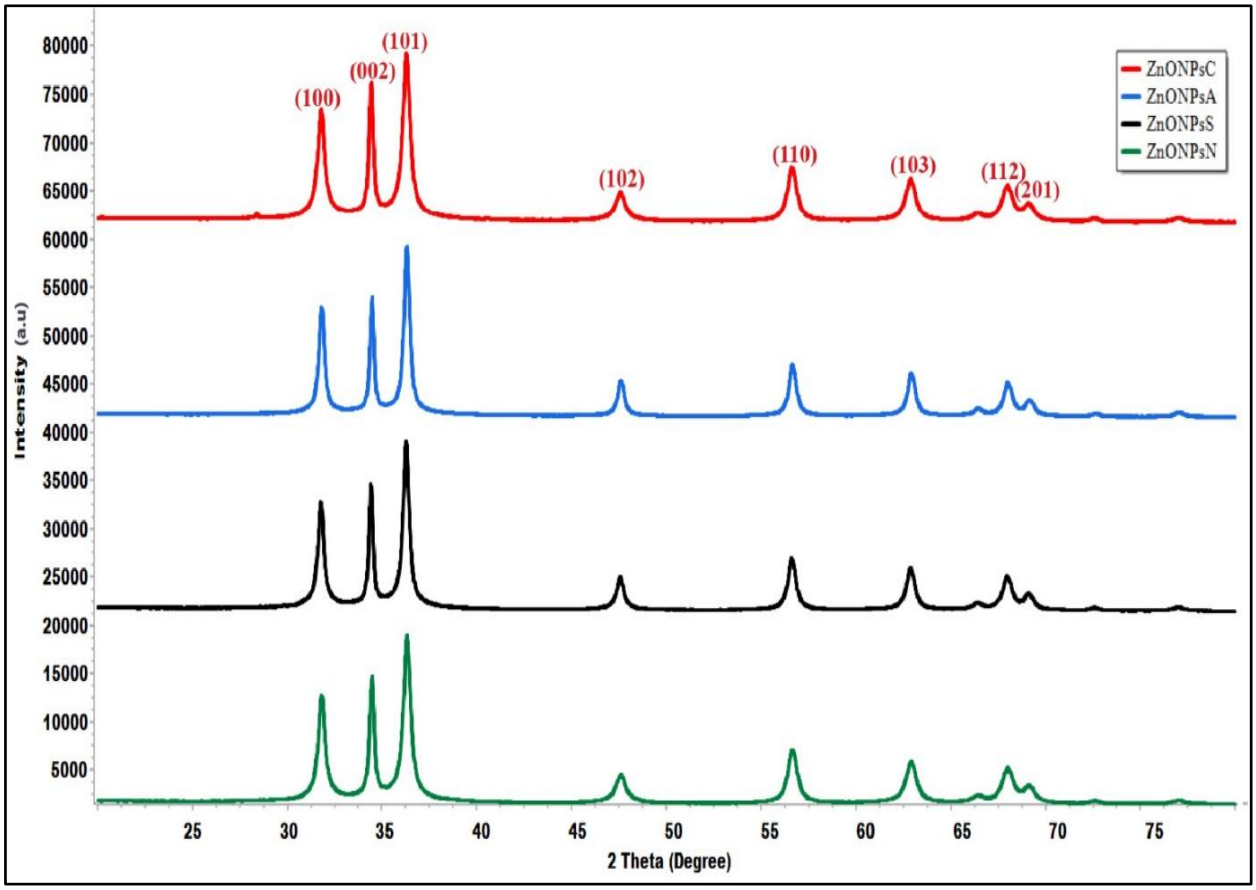

Figure 3. X-ray diffraction pattern of ZnONPsC, ZnONPsA, ZnONPsS and ZnONPsN.

Table 1. Average XRD crystallite size of the ZnONPs

Peak Number	Planes	2θ			
	hkl	ZnONPsC	ZnONPsA	ZnONPsS	ZnONPsN
1	100	31.8	31.82	31.78	31.82
2	002	34.44	34.48	34.43	34.48
3	101	36.29	36.31	36.28	36.32
4	102	47.57	47.60	47.57	47.6
5	110	56.63	56.65	56.61	56.66
6	103	62.88	62.91	62.87	62.91
7	112	67.98	67.99	67.95	68.01
8	201	69.10	69.14	69.10	69.14
Crystallite Size(nm)		20.04	22.09	24.34	21.38

3.4. FT-IR Results

Functional groups of phytochemicals responsible for the synthesis of ZnONPs were determined by FT-IR (Figure 4). The FTIR broad peak at 3400 cm^{-1} displayed in the spectra of Cinnamomum verum extract confirms the intermolecular hydrogen bonding. The FTIR bands for *Cinnamomum verum* extract recorded at 2353 cm^{-1}, 2148 cm^{-1}, and 1636 cm^{-1} indicate the presence C–H, N=N and C=C bendings respectively (Figure 4) (Baratta et al., 2003). The bands observed at 1191 cm^{-1} and 1118 cm^{-1} were assigned to alcohols and phenolic groups, C–N stretching vibrations of aliphatic and aromatic amines (Sangeetha et al., 2011). The band at 704 cm^{-1} is attributed to N−H deformation bands. Similar spectra were obtained for ZnONPs synthesized using Cinnamomum verum extract (Figure 4). The bands observed in the ranges of 3900-3700 cm^{-1}, 3500-3400 cm^{-1} and at approximately ~2900 cm^{-1} were assigned to O–H stretching of alcohols and C–H stretching of alkanes. In the spectrum of all ZnONPs,

the absorption peaks at approximately 1581-1572 cm^{-1} belong to C=C stretching and similarly, the absorption peaks at approximately 1407-1384 cm^{-1} belong to C–C stretching vibrations. These C=C stretching and C–C stretching vibrations are due to polyphenols responsible for the reduction and stabilization of NPs.The bands at around ~890 cm^{-1} are attributed to primary amine bands. The peaks in the region between around 600 cm−1 are assigned to ZnO (Figure 4) (Taş et al., 2000).

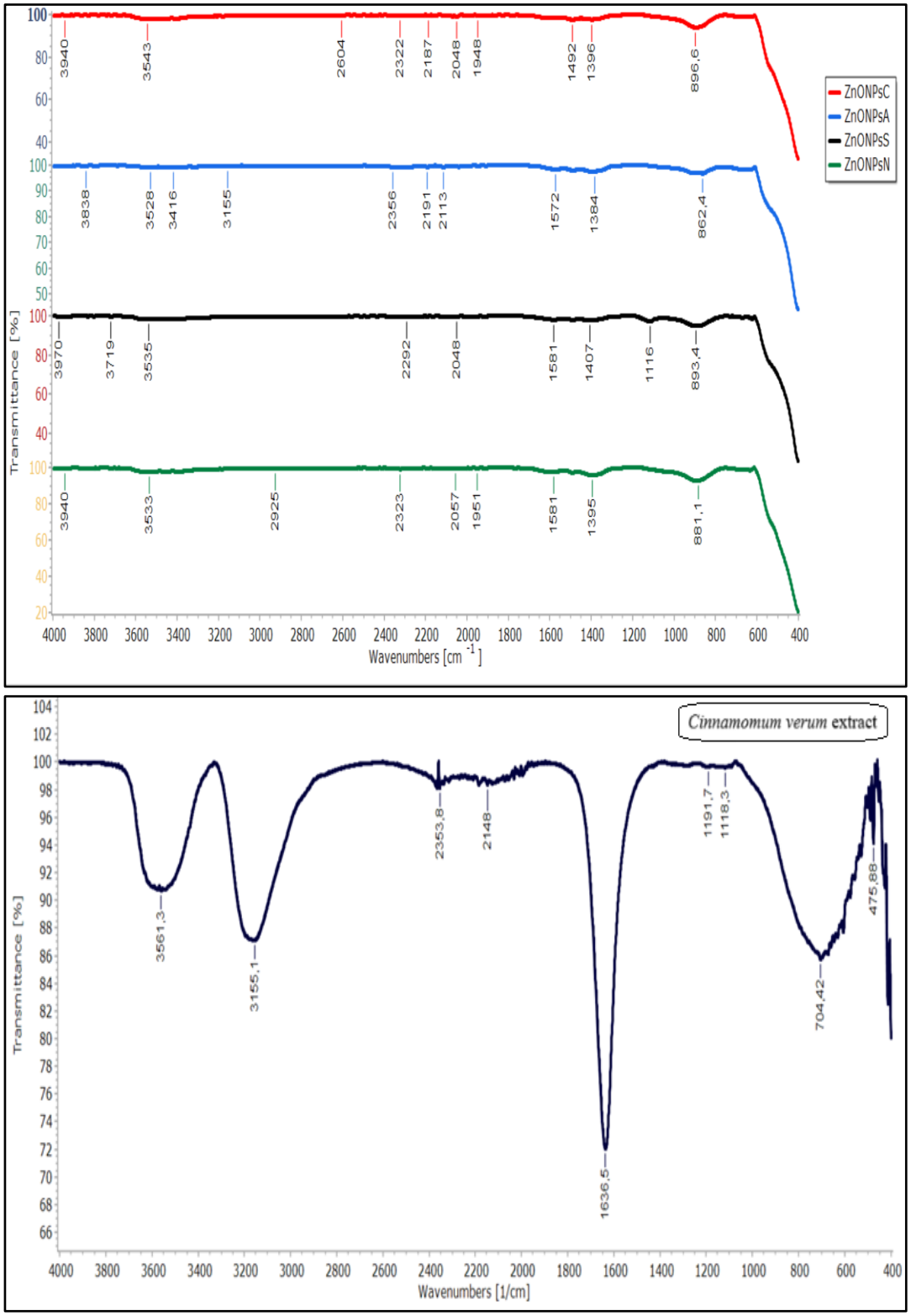

Figure 4. Fourier transform infrared pattern of ZnONPsC, ZnONPsA, ZnONPsS, ZnONPsN and Cinnamomum verum extract.

3.5. TEM results

TEM analysis was used to determine the morphologies and sizes of ZnONPs synthesized with different zinc salts (Figure 5). The results show that the significant impact of different zinc salts on the morphology and size of ZnONPs. ZnONPsC exhibited a mixture of rhombic, spherical, hexagonally clustered and wide-size distribution. ZnONPsA and ZnONPsS showed the formation of needle-shaped and flower-like structure morphology. This may be due to the ions promoting anisotropic growth. ZnONPsN produced more irregularly shaped such as spherical, nanorods nanoparticles with a broader size distribution ranging from 40 to 100 nm and some aggregation, due to the rapid release of nitrate ions which accelerates nucleation. This rapid nucleation might lead to less controlled growth, resulting in varied shapes and sizes. These findings demonstrate the significant effect of zinc salt type on the resulting morphology of zinc oxide nanoparticles. Previous studies have reported similar results (Mayekar, 2014; Shankar & Rhim, 2019; Abdelkader et al., 2022).

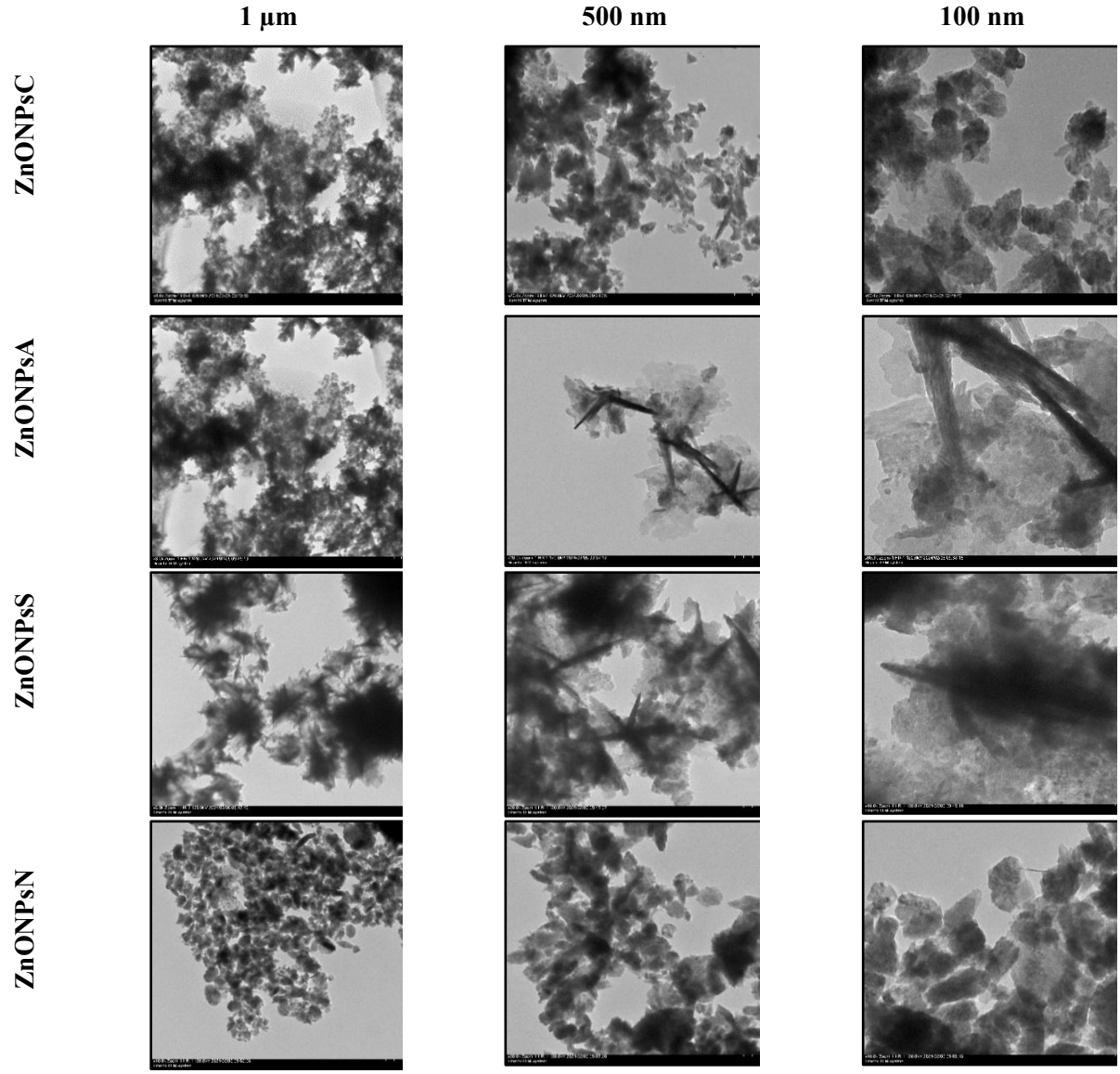

Figure 5. TEM images of ZnONPs synthesized from different zinc salts.

3.6. DLS and Zeta potentional results

Zeta potential and dynamic light scattering (DLS) analysis were used to determine the size distribution and surface charge properties of the nanoparticles**.** Zeta potential provides important information about the stability of nanoparticles. High zeta potential values (above +30 mV or below -30 mV) indicate strong repulsive forces between particles, indicating that the suspension is stable. Conversely, low zeta potential values increase the likelihood of particles coming closer together, leading to agglomeration or sedimentation (Rasmussen et al., 2020). According to the zeta potential results, ZnONPsS had the highest zeta potential value with −23± 0.7 mV (Figure 6c) followed by ZnONPsN with -22.7±0.7 Mv (Figure 6d). ZnONPsC zeta potential value was found to be 21.5±0.8 mV (Figure 6a). ZnONPsA showed the lowest zeta potential value at −9.56 ± 1.02 mV (Figure 6b). The zeta potential of nanoparticles is affected by their size, shape, surface functionalization, and chemical composition. Smaller nanoparticles and different geometries influence charge distribution, while modifications like chemical groups and coatings change surface charges, impacting the zeta potential (Leroy et al., 2011; Ovanesyan et al., 2016). Sulfate and nitrate ions, due to their high charge density, cause higher negative surface charges on the surface of the nanoparticles. These ions can bind more tightly on the surface of zinc oxide nanoparticles through electrostatic attraction, thereby increasing the surface charge density (Pourrahimi et al., 2014). Zinc acetate, zinc nitrate, zinc sulfate, and zinc chloride are all highly soluble in water. Specifically, zinc acetate has a solubility of approximately 430 g/L, zinc sulfate about 540 g/L, zinc nitrate around 1840 g/L, and zinc chloride has an extremely high solubility of approximately 4320 g/L. It was observed that nanoparticles synthesized from zinc chloride had a high size distribution (Table 2). In general, the nanoparticle size distribution increased due to the increase in the solubility of the salts (ZnONPsA<ZnONPsN <ZnONPsS <ZnONPsC). The high solubility of zinc salt can further accelerate nucleation, reduce control over particle growth, and cause a wider distribution of particle sizes and more aggregation. Another important factor in DLS analysis is the polydispersity index (PDI). PDI is a critical parameter to determine the homogeneity of the size distribution of particles. A PDI value between 0.05 and 0.7 indicates a monodisperse particle size distribution, while a value greater than 0.7 indicates a broad particle size distribution (Danaei et al., 2018). According to the results in Table 2, the PDI value of the nanoparticles is ZnONPsA < ZnONPsC < ZnONPsN < ZnONPsS. However, only ZnONPsS was found to have a broad size distribution with a value greater than 0.7.

Table 2. Zeta potential value and size distribution of ZnONPs synthesized from different zinc salts

Samples	T (°C)	Z-Ave (nm)	PdI	ZP (mV)	Mobility (µmcm/Vs)	Conductivity (mS/cm)
ZnONPsC	25	1866	0,518	-21,5	-1,686	0,00811
ZnONPsA	25	400,6	0,376	-9,56	-0,7505	0,00978
ZnONPsS	25	880,4	0,725	-23	-1,8	0,00539
ZnONPsN	25	802,3	0,53	-22,7	-1,782	0,00798

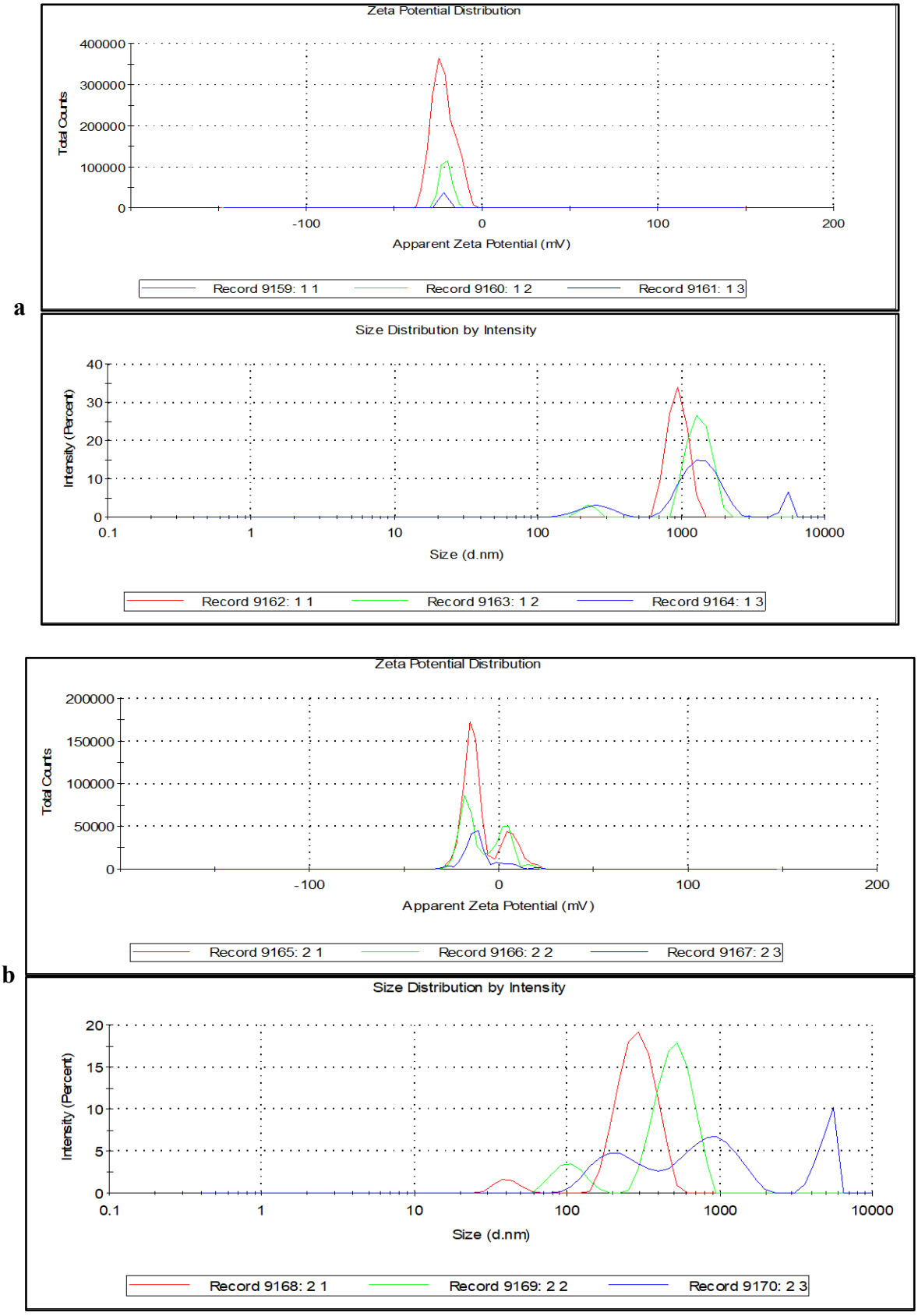

Figure 6. Zeta potential and size distribution graphs of ZnO NOPs synthesized from different zinc salts a) ZnONPsC b) ZnONPsA c) ZnONPsS d) ZnONPsN.

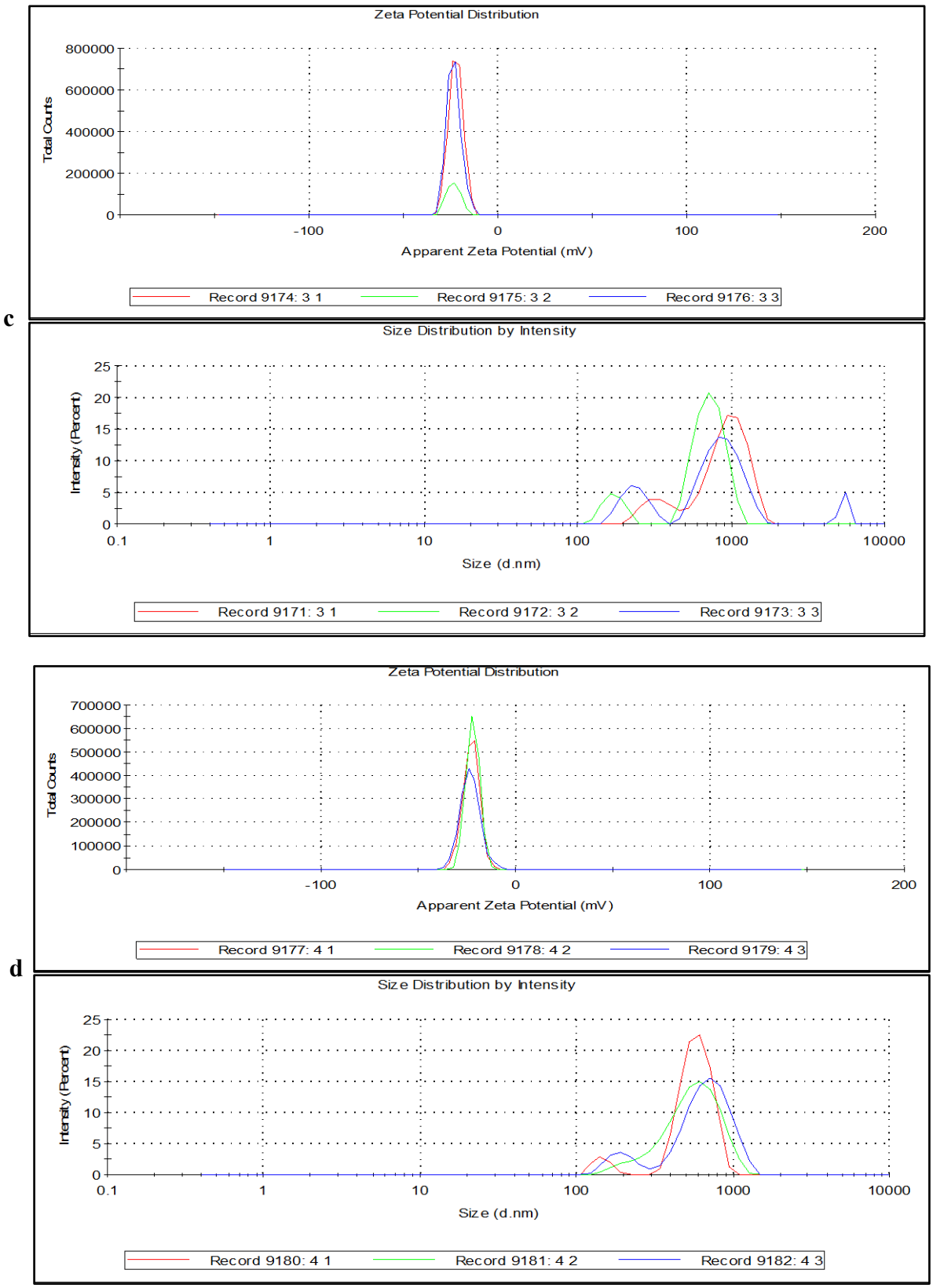

Figure 6. Zeta potential and size distribution graphs of ZnO NOPs synthesized from different zinc salts a) ZnONPsC b) ZnONPsA c) ZnONPsS d) ZnONPsN (continue).

3.7. Effect of ZnO nanoparticle on photodegradation of MB

The effect on the photocatalytic efficiency of ZnONPs synthesized using different salts is presented in the graph in the presence and absence of sunlight (Figure 7). The percentage of photodegradation in the absence of sunlight is significantly lower for all samples than in the presence of sunlight. The Photocatalytic activity in the presence of sunlight is relatively high for all samples, indicating the effectiveness of the ZnO nanoparticles under photocatalytic conditions. ZnONPC has the highest removal efficiency in sunlight (79.431%), closely followed by ZnONPN (78.976%). The Photocatalytic activity of absence sunlight is much lower, with ZnONP A showing the highest removal (20.88%) and ZnONP N the lowest (3.43%). The increase in crystallite size, calculated from XRD data, results in a higher available surface area for the adsorption of more oxygen and the photogeneration of more electrons and holes (Steffy et al., 2018). Various factors affect the photocalytic activity of the material, including surface area, particle size, adsorption, and calcination temperature (Gaim et al., 2019). The differences in crystallite size among the samples do not appear to significantly impact their efficiency in sunlight, although there is a noticeable variance in their performance in the absence of sunlight. The data suggests that ZnO nanoparticles are highly effective as photocatalysts for dye removal when exposed to sunlight. Addinatily, photochemicals transferred fromplant extracts during biosynthesis may be effective in the formation of radicals required for the photocatalytic degradation of MB.

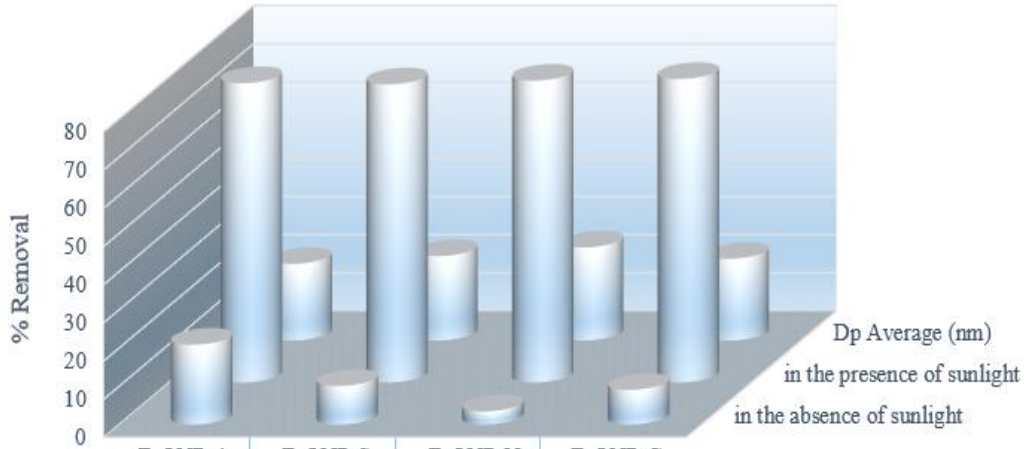

	ZnONPsA	ZnONPsS	ZnONPsN	ZnONPsC
in the absence of sunlight	20,88	10,08	3,43	9,066
in the presence of sunlight	78,337	78,0147	78,976	79,431
Dp Average (nm)	20,04	22,09	24,34	21,38

Figure 7. Photodegradability of MB dye by the ZnONPs catalyst in the presence and absence of sunlight.

4. Conclusion

In this research, ZnONPs were successfully biosynthesized using *Cinnamomum verum* extract and a unique eco-friendly route was provided to synthesize ZnO NPs with size and morphology characteristics using different zinc salts (zinc acetate, zinc nitrate, zinc sulfate and zinc chloride). XRD, DLS, FT-IR and TEM confirmed that the different zinc salts used in the synthesis process significantly affect the morphology, size and crystal structure of the resulting nanoparticles. Zinc chloride salts synthesized rhombic, spherical and hexagonally clustered ZnONPs with a wide size distribution. At the same time, zinc acetate and zinc sulfate formed needle-shaped and flower-like structures, respectively, probably due to the ions promoting anisotropic growth. Additionally, nitrate salt produced more irregularly shaped nanoparticles, such as spherical and nanorods, with a wider size distribution. All ZnONPs exhibited similar crystal structures with different sizes. Different zinc salts are critical in determining the characteristics and effectiveness of ZnO nanoparticles. ZnONPsA showed the highest photocatalytic efficiency in degrading methylene blue (MB) dy*e*. In particular, needle-shaped and

flower-like ZnO particles were found to exhibit a remarkable efficiency increase compared to spherical particles. It was observed that the photocatalytic efficiency was not affected by the size of ZnO particles, but the geometrical factor was significant. Additionally, *Cinnamomum verum* extract has been found to have strong antioxidant properties by DPPH testing and total phenolic content analysis. Synthesized through a green, biogenic method. This study highlights the synthesis of ZnO nanoparticles with an environmentally friendly method and the importance of their applications in biomedical fields. Moreover, the photocatalytic ability of ZnO nanoparticles can be exploited in environmental protection strategies.

Author Contributions

The first and second authors conceived the main conceptual ideas. The first author performed the experiment. The second author wrote the article with the support of the first author. All authors read and approved the final version of the paper.

Conflicts of Interest

All the authors declare no conflict of interest.

Acknowledgement

This research did not receive any funding. We acknowledge the author for their contributions

References

Abdelkader, D. H., Negm, W. A., Elekhnawy, E., Eliwa, D., Aldosari, B. N., & Almurshedi, A. S. (2022). Zinc Oxide nanoparticles as potential delivery carrier: Green synthesis by aspergillus niger endophytic fungus, characterization, and ın vitro/ın vivo antibacterial activity. *Pharmaceuticals*, *15*(9). https://doi.org/10.3390/ph15091057

Abdullah, J. A. A., Guerrero, A., & Romero, A. (2024). efficient and sustainable synthesis of zinc salt-dependent polycrystal zinc oxide nanoparticles: comprehensive assessment of physicochemical and functional properties. *Applied Sciences (Switzerland)*, *14*(5). https://doi.org/10.3390/app14051815

Abeysekera, W. P. K. M., Premakumara, G. A. S., & Ratnasooriya, W. D. (2013). In vitro antioxidant properties of leaf and bark extracts of ceylon cinnamon (cinnamomum zeylanicum blume). *Tropical Agricultural Research, 24*(2), 128-138.

Aigbe, U. O., & Osibote, O. A. (2024). Green synthesis of metal oxide nanoparticles, and their various applications. *Journal of Hazardous Materials Advances*, *13*(January), 100401. https://doi.org/10.1016/j.hazadv.2024.100401

Aydoğdu, B., Aytar, M., & Ünal, İ. (2024). Comparison of characteristics and antimicrobial activity of synthesized zinc oxide and magnetite ıron oxide nanoparticles using four different plant extracts. *Cumhuriyet Science Journal*, *45*(1), 20–28. https://doi.org/10.17776/csj.1370606

Baratta, G. A., Domingo, M., Ferini, G., Leto, G., Palumbo, M. E., Satorre, M. A., & Strazzulla, G. (2003). Ion irradiation of CH4-containing icy mixtures. *Nuclear Instruments and Methods in Physics Research, Section B: Beam Interactions with Materials and Atoms*, *209*(August), 283–287. https://doi.org/10.1016/S0168-583X(02)02010-4

Bhandari, K. P., Sapkota, D. R., Jamarkattel, M. K., Stillion, Q., & Collins, R. W. (2023). Zinc oxide nanoparticles—solution-based synthesis and characterizations. *Nanomaterials*, *13*(11). https://doi.org/10.3390/nano13111795

Błaszczyk, N., Rosiak, A., & Kałużna-Czaplińska, J. (2021). The potential role of cinnamon in human health. *Forests*, *12*(5), 1–17. https://doi.org/10.3390/f12050648

Danaei, M., Dehghankhold, M., Ataei, S., Hasanzadeh Davarani, F., Javanmard, R., Dokhani, A., Khorasani, S., & Mozafari, M. R. (2018). Impact of particle size and polydispersity index on the clinical applications of lipidic nanocarrier systems. *Pharmaceutics, 10*(2), 57. https://doi.org/10.3390/pharmaceutics10020057

Das, G., Gonçalves, S., Basilio Heredia, J., Romano, A., Jiménez-Ortega, L. A., Gutiérrez-Grijalva, E. P., Shin, H. S., & Patra, J. K. (2022). Cardiovascular protective effect of cinnamon and its major bioactive constituents: An update. *Journal of Functional Foods*, *97*(January 2023). https://doi.org/10.1016/j.jff.2022.105045

Fahmy, M. D., Jazayeri, H. E., Razavi, M., Hashemi, M., Omidi, M., Farahani, M., Salahinejad, E., Yadegari, A., Pitcher, S., & Tayebi, L. (2016). Biomedical Applications of Intelligent Nanomaterials. *Intelligent Nanomaterials: Second Edition*, *13*(10), 199–245. https://doi.org/10.1002/9781119242628.ch8

Fito, J., Abewaa, M., Mengistu, A., Angassa, K., Ambaye, A. D., Moyo, W., & Nkambule, T. (2023). Adsorption of methylene blue from textile industrial wastewater using activated carbon developed from Rumex abyssinicus plant. *Scientific Reports*, *13*(1), 1–17. https://doi.org/10.1038/s41598-023-32341-w

Gaim, Y. T., Tesfamariam, G. M., Nigussie, G. Y., & Ashebir, M. E. (2019). Synthesis, characterization and photocatalytic activity of n-doped cu2o/zno nanocomposite on degradation of methyl red. *Journal of Composites Science*, *3*(4). https://doi.org/10.3390/jcs3040093

Iravani, S., Korbekandi, H., Mirmohammadi, S. V., & Zolfaghari, B. (2014). Synthesis of silver nanoparticles: chemical, physical and biological methods. *Research in Pharmaceutical Sciences*, *9*(6), 385–406.

Kazemi, S., Hosseingholian, A., Gohari, S. D., Feirahi, F., Moammeri, F., Mesbahian, G., Moghaddam, Z. S., & Ren, Q. (2023). Recent advances in green synthesized nanoparticles: from production to application. *Materials Today Sustainability*, *24*, 100500. https://doi.org/10.1016/j.mtsust.2023.100500

Kedare, S. B., & Singh, R. P. (2011). Genesis and development of DPPH method of antioxidant assay. *Journal of Food Science and Technology*, *48*(4), 412–422. https://doi.org/10.1007/s13197-011-0251-1

Khan, I., Saeed, K., & Khan, I. (2019). Nanoparticles: Properties, applications and toxicities. *Arabian Journal of Chemistry*, *12*(7), 908–931. https://doi.org/10.1016/j.arabjc.2017.05.011

Kulkarni, D., Sherkar, R., Shirsathe, C., Sonwane, R., Varpe, N., Shelke, S., More, M. P., Pardeshi, S. R., Dhaneshwar, G., Junnuthula, V., & Dyawanapelly, S. (2023). Biofabrication of nanoparticles: sources, synthesis, and biomedical applications. *Frontiers in Bioengineering and Biotechnology*, *11*(May), 1–26. https://doi.org/10.3389/fbioe.2023.1159193

Leroy, P., Tournassat, C., & Bizi, M. (2011). Influence of surface conductivity on the apparent zeta potential of TiO2 nanoparticles. *Journal of Colloid and Interface Science*, *356*(2), 442–453. https://doi.org/10.1016/j.jcis.2011.01.016

Libbey, L. M., & Walradt, J. P. (1968). 3,5-di-Tert-butyl-4-hydroxytoluene (BHT) as an artifact from diethyl ether. *Lipids*, *3*(6), 561. https://doi.org/10.1007/BF02530903

Marin-Flores, C. A., Rodríguez-Nava, O., García-Hernández, M., Ruiz-Guerrero, R., Juárez-López, F., & Morales-Ramírez, A. de J. (2021). Free-radical scavenging activity properties of ZnO sub-micron particles: size effect and kinetics. *Journal of Materials Research and Technology*, *13*, 1665–1675. https://doi.org/10.1016/j.jmrt.2021.05.050

Mayekar, J. (2014). Role of salt precursor in the synthesis of zınc oxide nanoparticles. *International Journal of Research in Engineering and Technology*, *03*(03), 43–45. https://doi.org/10.15623/ijret.2014.0303008

Naiel, B., Fawzy, M., Halmy, M. W. A., & Mahmoud, A. E. D. (2022). Green synthesis of zinc oxide nanoparticles using Sea Lavender (Limonium pruinosum L. Chaz.) extract: characterization, evaluation of anti-skin cancer, antimicrobial and antioxidant potentials. *Scientific Reports*, *12*(1), 1–12. https://doi.org/10.1038/s41598-022-24805-2

Nyabadza, A., McCarthy, É., Makhesana, M., Heidarinassab, S., Plouze, A., Vazquez, M., & Brabazon, D. (2023). A review of physical, chemical and biological synthesis methods of bimetallic nanoparticles and applications in sensing, water treatment, biomedicine, catalysis and hydrogen storage. *Advances in Colloid and Interface Science*, *321*(August). https://doi.org/10.1016/j.cis.2023.103010

Osman, A. I., Zhang, Y., Farghali, M., Rashwan, A. K., Eltaweil, A. S., Abd El-Monaem, E. M., Mohamed, I. M. A., Badr, M. M., Ihara, I., Rooney, D. W., & Yap, P. S. (2024). Synthesis of green nanoparticles for energy, biomedical, environmental, agricultural, and food applications: A review. *Environmental Chemistry Letters, 22*(2), 841-887. https://doi.org/10.1007/s10311-023-01682-3

Ovanesyan, Z., Aljzmi, A., Almusaynid, M., Khan, A., Valderrama, E., Nash, K. L., & Marucho, M. (2016). Ion-ion correlation, solvent excluded volume and pH effects on physicochemical properties of spherical oxide nanoparticles. *Journal of Colloid and Interface Science*, *462*, 325–333. https://doi.org/10.1016/j.jcis.2015.10.019

Pourrahimi, A. M., Liu, D., Pallon, L. K. H., Andersson, R. L., Martínez Abad, A., Lagarón, J. M., Hedenqvist, M. S., Ström, V., Gedde, U. W., & Olsson, R. T. (2014). Water-based synthesis and cleaning methods for high purity ZnO nanoparticles-comparing acetate, chloride, sulphate and nitrate zinc salt precursors. *RSC Advances*, *4*(67), 35568–35577. https://doi.org/10.1039/c4ra06651k

Prabu, P., & Losetty, V. (2024). Green synthesis of copper oxide nanoparticles using Macroptilium Lathyroides (L) leaf extract and their spectroscopic characterization, biological activity and photocatalytic dye degradation study. *Journal of Molecular Structure*, *1301*(August 2023), 137404. https://doi.org/10.1016/j.molstruc.2023.137404

Prasad, C., Liu, Q., Tang, H., Yuvaraja, G., Long, J., Rammohan, A., & Zyryanov, G. V. (2020). An overview of graphene oxide supported semiconductors based photocatalysts: Properties, synthesis and photocatalytic applications. *Journal of Molecular Liquids, 297,* 111826. https://doi.org/10.1016/j.molliq.2019.111826

Rasmussen, M. K., Pedersen, J. N., & Marie, R. (2020). Size and surface charge characterization of nanoparticles with a salt gradient. *Nature Communications*, *11*(1), 1–8. https://doi.org/10.1038/s41467-020-15889-3

Rezapour, M., & Talebian, N. (2011). Comparison of structural, optical properties and photocatalytic activity of ZnO with different morphologies: Effect of synthesis methods and reaction media. *Materials Chemistry and Physics*, *129*(1–2), 249–255. https://doi.org/10.1016/j.matchemphys.2011.04.012

Saeed, K., Khan, I., Shah, T., & Park, S. Y. (2015). Synthesis, characterization and photocatalytic activity of silver nanoparticles/amidoxime-modified polyacrylonitrile nanofibers. *Fibers and Polymers*, *16*(9), 1870–1875. https://doi.org/10.1007/s12221-015-5373-z

Sajid, M., & Płotka-Wasylka, J. (2020). Nanoparticles: Synthesis, characteristics, and applications in analytical and other sciences. *Microchemical Journal*, *154*(November 2019), 104623. https://doi.org/10.1016/j.microc.2020.104623

Sangeetha, G., Rajeshwari, S., & Venckatesh, R. (2011). Green synthesis of zinc oxide nanoparticles by aloe barbadensis miller leaf extract: Structure and optical properties. *Materials Research Bulletin*, *46*(12), 2560–2566. https://doi.org/10.1016/j.materresbull.2011.07.046

Saod, W. M., Al-Janaby, M. S., Gayadh, E. W., Ramizy, A., & Hamid, L. L. (2024). Biogenic synthesis of iron oxide nanoparticles using Hibiscus sabdariffa extract: Potential for antibiotic development and antibacterial activity against multidrug-resistant bacteria. *Current Research in Green and Sustainable Chemistry*, *8*(January), 100397. https://doi.org/10.1016/j.crgsc.2024.100397

Shankar, S., & Rhim, J. W. (2019). Effect of Zn salts and hydrolyzing agents on the morphology and antibacterial activity of zinc oxide nanoparticles. *Environmental Chemistry Letters*, *17*(2), 1105–1109. https://doi.org/10.1007/s10311-018-00835-z

Sirelkhatim, A., Mahmud, S., Seeni, A., Kaus, N. H. M., Ann, L. C., Bakhori, S. K. M., Hasan, H., & Mohamad, D. (2015). Review on zinc oxide nanoparticles: Antibacterial activity and toxicity mechanism. *Nano-Micro Letters*, *7*(3), 219–242. https://doi.org/10.1007/s40820-015-0040-x

Song, F. L., Gan, R. Y., Zhang, Y., Xiao, Q., Kuang, L., & Li, H. B. (2010). Total phenolic contents and antioxidant capacities of selected chinese medicinal plants. *International Journal of Molecular Sciences*, *11*(6), 2362–2372. https://doi.org/10.3390/ijms11062362

Steffy, K., Shanthi, G., Maroky, A. S., & Selvakumar, S. (2018). Synthesis and characterization of ZnO phytonanocomposite using Strychnos nux-vomica L. (Loganiaceae) and antimicrobial activity against multidrug-resistant bacterial strains from diabetic foot ulcer. *Journal of Advanced Research*, *9*, 69–77. https://doi.org/10.1016/j.jare.2017.11.001

Sudan, R., Bhagat, M., Gupta, S., Chitrarakha, & Devi, T. (2013). Comparative analysis of cytotoxic and antioxidant potential of edible Cinnamomum verum (bark) and Cinnamomum tamala (Indian bay leaf). *Free Radicals and Antioxidants, 3*(2), 70-73. https://doi.org/10.1016/j.fra.2013.05.005

Talam, S., Karumuri, S. R., & Gunnam, N. (2012). Synthesis, Characterization, and Spectroscopic Properties of ZnO Nanoparticles. *ISRN Nanotechnology*, *2012*, 1–6. https://doi.org/10.5402/2012/372505

Tănase, M. A., Marinescu, M., Oancea, P., Răducan, A., Mihaescu, C. I., Alexandrescu, E., Nistor, C. L., Jinga, L. I., Diţu, L. M., Petcu, C., & Cinteza, L. O. (2021). Antibacterial and photocatalytic properties of ZnO nanoparticles obtained from chemical versus Saponaria officinalis extract-mediated synthesis. *Molecules*, *26*(7), 2072. https://doi.org/10.3390/molecules26072072

Taş, A. C., Majewski, P. J., & Aldinger, F. (2000). Chemical preparation of pure and strontium- and/or magnesium-doped lanthanum gallate powders. *Journal of the American Ceramic Society*, *83*(12), 2954–2960. https://doi.org/10.1111/j.1151-2916.2000.tb01666.x

Venkatesan, S., Suresh, S., Ramu, P., Arumugam, J., Thambidurai, S., & Pugazhenthiran, N. (2022). Methylene blue dye degradation potential of zinc oxide nanoparticles bioreduced using Solanum trilobatum leaf extract. *Results in Chemistry*, *4*(September), 100637. https://doi.org/10.1016/j.rechem.2022.100637

Zhou, X. Q., Hayat, Z., Zhang, D. D., Li, M. Y., Hu, S., Wu, Q., Cao, Y. F., & Yuan, Y. (2023). Zinc Oxide Nanoparticles: Synthesis, Characterization, Modification, and Applications in Food and Agriculture. *Processes*, *11*(4), 1193. https://doi.org/10.3390/pr11041193

Zuhrotun, A., Oktaviani, D. J., & Hasanah, A. N. (2023). Biosynthesis of gold and silver nanoparticles using phytochemical compounds. *Molecules*, *28*(7), 3240. https://doi.org/10.3390/molecules28073240